Metallic conduction at organic charge-transfer interfaces

HELENA ALVES, ANNA S. MOLINARI, HANGXING XIE AND ALBERTO F. MORPURGO*

Kavli Institute of Nanoscience, Delft University of Technology, Lorentzweg 1, 2628 CJ Delft, The Netherlands

*e-mail: A.Morpurgo@tudelft.nl

Published online: 15 June 2008; doi:10.1038/nmat2205

The electronic properties of interfaces between two different solids can differ strikingly from those of the constituent materials. For instance, metallic conductivity—and even superconductivity—have recently been discovered at interfaces formed by insulating transition-metal oxides. Here, we investigate interfaces between crystals of conjugated organic molecules, which are large-gap undoped semiconductors, that is, essentially insulators. We find that highly conducting interfaces can be realized with resistivity ranging from 1 to 30 kΩ per square, and that, for the best samples, the temperature dependence of the conductivity is metallic. The observed electrical conduction originates from a large transfer of charge between the two crystals that takes place at the interface, on a molecular scale. As the interface assembly process is simple and can be applied to crystals of virtually any conjugated molecule, the conducting interfaces described here represent the first examples of a new class of electronic systems.

Many times in the past, the discovery of metallic electrical conductivity in molecular-based materials has led to the development of new fields of research. Well-known examples are iodine doping of polyacetylene[1], which started the field of polymer electronics, alkali intercalation of the fullerenes[2], with the subsequent discovery of superconductivity[3], and the development of charge-transfer salts[4], in which a cornucopia of phenomena originating from electron–electron and electron–phonon interactions has been observed. All of this work has been confined to bulk compounds and the realization of metallic conductivity at the surface of molecular-based materials has so far been much less successful (for very promising recent work in this direction, see ref. 5). This is unfortunate, because the very rich electronic properties of surfaces and interfaces can enable the observation of new physical phenomena. In inorganic materials, for instance, this is illustrated by the discovery of metallicity[6]—and even superconductivity[7] and magnetism[8]—at interfaces between different insulating, non-magnetic transition-metal oxides. Here, we show that a metallic system can also be created at the interface between crystals of two different conjugated organic molecules, which are both insulators in the bulk.

The molecules that we have selected for our study are tetrathiofulvalene (TTF) and 7,7,8,8-tetracyanoquinodimethane (TCNQ), which are famous for their use in the synthesis of the first metallic organic charge-transfer compound[9]. In such a compound, TTF and TCNQ are arranged in linear chains, forming a well-defined crystalline structure (Fig. 1). Electrons in the highest occupied molecular orbital (HOMO) of TTF are transferred to the lowest unoccupied molecular orbital (LUMO) of TCNQ, with virtually no hybridization between the molecular levels. As a result, the TTF and TCNQ chains behave as decoupled, one-dimensional electronic systems, and at room temperature the material is highly conducting. At low temperature, the compound becomes an insulator owing to two Peierls transitions occurring independently on the TTF and TCNQ chains (at $T = 54$ K for the TCNQ chain and $T = 38$ K for the TTF chain), a clear manifestation of the underlying one-dimensionality of the material (for a review, see refs 10,11).

Rather than focusing on bulk TTF–TCNQ, we have investigated electronic transport at the interface between TTF and TCNQ crystals. As shown in Fig. 2, TTF and TCNQ crystals are semiconductors, with electronic properties that are similar to those of many other organic materials (for example, pentacene) commonly used in the field of plastic electronics, for instance for the fabrication of flexible field-effect transistors (FETs). The bandgap in these materials is approximately equal to the HOMO–LUMO gap of the corresponding molecule, which is larger than 2 eV (ref. 12). As a consequence, the conductivity of pure TTF and TCNQ crystals is vanishingly small.

It is not *a priori* clear whether, similarly to the case of the bulk, charge transfer between the two molecules can indeed take place at a TTF–TCNQ interface. For this to happen, the energy of the charge-transfer state ($D^{\bullet+}A^{\bullet-}$, where D stands for donor and A for acceptor) has to be smaller than the energy of the system when the molecules remain neutral (D^0A^0). The energetic balance is determined by the difference in the energy of the TTF HOMO and the TCNQ LUMO—which is similar in the bulk and at the interface—and by the Coulomb energy stored in the charge-transfer state, which is larger for a planar two-dimensional interface as compared with the interpenetrating linear chains present in the TTF–TCNQ bulk. It may therefore be that the extra cost in Coulomb energy prevents the occurrence of a large charge transfer. In addition, next to these fundamental aspects, technological problems may also prevent the assembly of a sufficiently ideal TTF–TCNQ interface. For instance, TTF–TCNQ interfaces may be unstable against mutual interdiffusion of the two molecular species (a solid-state reaction between TTF and TCNQ could occur, resulting in bulk TTF–TCNQ[13]), or imperfection present at the crystal surfaces may trap all transferred charge.

The assembly of the TTF–TCNQ interfaces is done manually, in air, by first placing a TCNQ crystal onto a soft polydimethylsiloxane (PDMS) stamp, and by subsequently laminating a TTF crystal on

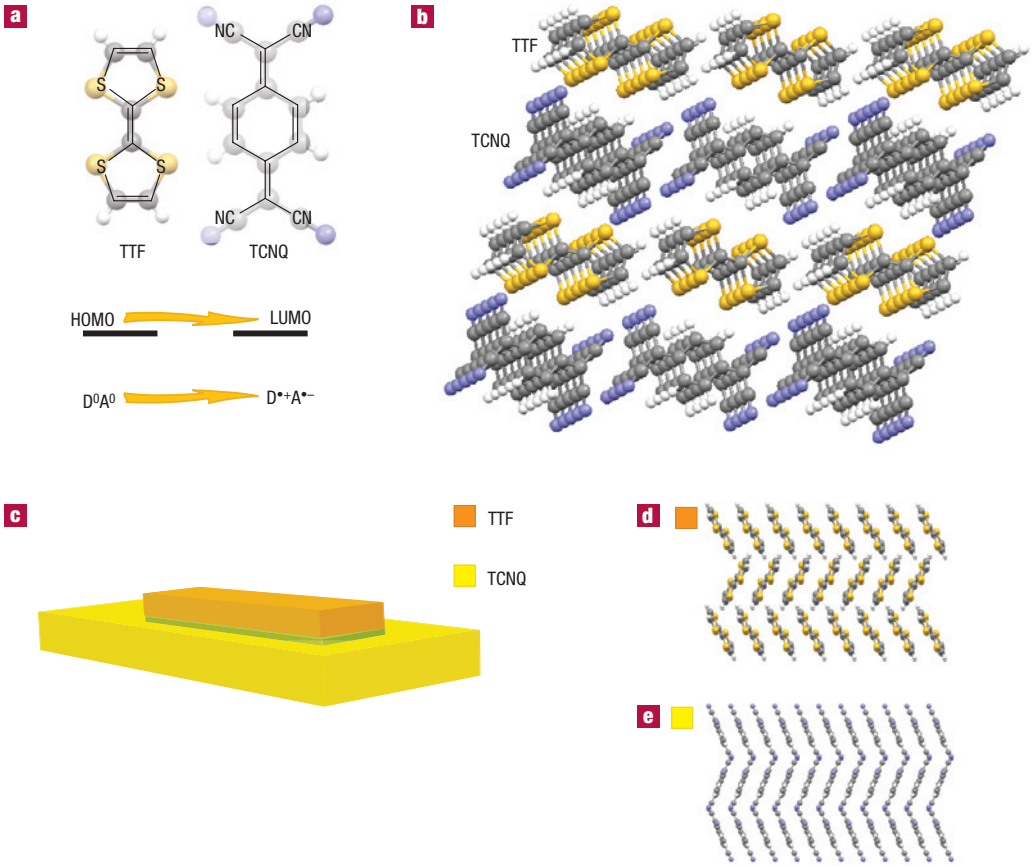

Figure 1 Charge transfer in the TTF–TCNQ system. ab, The TTF and TCNQ molecules (**a**) are well known since their use in the synthesis of the first metallic charge-transfer compound, TTF–TCNQ, the structure of which (**b**) (ref. 34) consists of a quasi-one-dimensional, chain-like arrangement of the TTF and TCNQ molecules. In TTF–TCNQ crystals, electrons from the HOMO of the TTF molecules are transferred into the LUMO of the TCNQ molecules, leading to a stable charge-transfer state (as indicated in the diagram in **a**). **c**, Our work investigates whether a similar charge transfer occurs at the interface between a TTF and TCNQ crystal (green shaded region), leading to the occurrence of a metallic state. **d**,**e**, Top view of the structure of the molecular planes (note the characteristic herringbone configuration) where conduction takes place in (α-phase) TTF (**d**) (ref. 35) and TCNQ (**e**) (ref. 36). In our samples, these molecular planes are parallel to (and form) the TTF–TCNQ interface. All structures shown are courtesy of the Cambridge Structural Database.

top of TCNQ. The different steps involved are shown in Fig. 3. This lamination technique has been used extensively over the past years for the study of organic single-crystal FETs (ref. 14), the fabrication of which relies on the fact that thin organic single crystals of conjugated molecules adhere to the surface of virtually any insulating and metallic material. For instance, crystals of polyacenes (anthracene[15], tetracene[16], pentacene[17]), rubrene[18], metal phthalocyanines[19], thiophenes[20] and many other molecules adhere easily onto insulators such as SiO_2, Ta_2O_5, HfO_2, Al_2O_3, Si_3N_4 and PDMS[18,21], or onto metal films of Au, Pt, Ni, Cu and Co (ref. 22). Organic single crystals also adhere spontaneously to molecular materials, such as self-assembled monolayers[17], polymethylmethacrylate[23] or other organic crystals. Recently, for instance, crystals of diphenylanthracene, which has a large HOMO–LUMO gap, have been laminated onto rubrene crystals and used as a gate dielectric[24]. In all cases, adhesion occurs when the surface of the crystals is sufficiently flat, which is the case for most organic molecules[25] (for the substrate, the roughness typically has to be smaller than a few nanometres), and when crystals are sufficiently flexible to conform to the surface to which they are bonded. This is the case for ~1-μm-thick crystals (similar to those used in this work), with the precise thickness being dependent on the molecular material. The mechanism responsible for the adhesion is not known in detail, but there is a wide consensus that the ubiquity of the phenomenon (the insensitivity to the materials used) points to electrostatic attraction (for example, van der Waals forces), and that chemistry at the interface does not play a relevant role[14]. For the work presented here, it is particularly important that electrostatic bonding of organic crystals permits the reproducible fabrication of very high-quality devices without introducing damage to the surface of the organic material[26], as demonstrated by a number of experiments. For instance, rubrene FETs fabricated by lamination have led to the discovery that, for high-dielectric-constant insulators, charge carriers in rubrene interact strongly with the self-polarization cloud in the insulator, resulting in the formation of interfacial Frohlich polarons[18]. Crystal lamination has also enabled reproducible contact resistance in organic transistors with nickel electrodes, with record-low values[27] (100 Ω cm). However, the operation of single-crystal devices studied so far did not rely on the occurrence of charge transfer between two different materials, and it remains to be seen whether in-air crystal lamination can also be used for the assembly of the TTF–TCNQ interfaces that we are interested in.

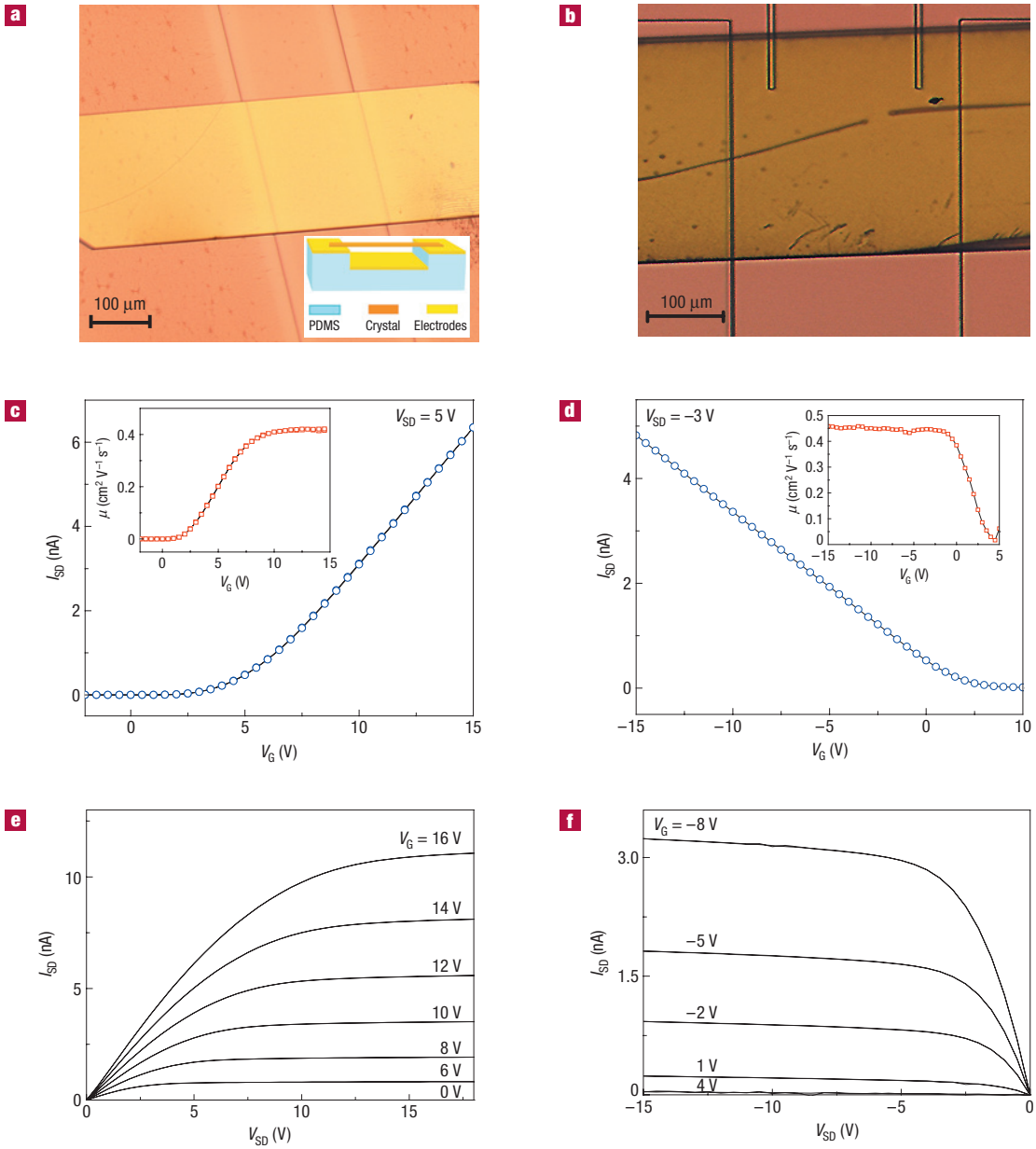

Figure 2 Characterization of TCNQ and TTF single crystals. The electrical characterization of the TCNQ and TTF single crystals used in the assembly of TTF–TCNQ interfaces relies on the use of FETs. The devices are fabricated by laminating a single crystal onto a so-called PDMS air-gap stamp, as shown in the inset of **a** (for technical details, see ref. 37). **a**,**b**, Optical microscope image of a single-crystal TCNQ (**a**) and TTF (**b**) FET. **c**,**d**, The source drain current I_{SD} measured on one of our TCNQ (**c**) and TTF (**d**) devices as a function of gate voltage and for a fixed source drain bias ($V_{SD} = 5$ V for the TCNQ device and $V_{SD} = -3$ V for the TTF device). As expected for TCNQ—which is an electron acceptor—the current increases for positive gate voltages, that is, when electrons are accumulated in the channel. In the off state (negative gate voltages), the device resistance is much larger than 1 GΩ, as expected because TCNQ crystals are undoped, large-gap semiconductors. The inset shows the electron mobility of the same device obtained by numerically deriving the $I(V)$ curve. Electron mobility values as high as 2 $cm^2 V^{-1} s^{-1}$ have been observed in vapour-phase-grown TCNQ single crystals (see, for example, ref. 37); the value here is lower, probably because a non-negligible contact resistance at the source and drain electrodes is present in our two-terminal configuration. **e**,**f**, The transfer curves of the TCNQ (**e**) and TTF (**f**) device measured at different gate voltages, with the TCNQ device showing ideal transistor characteristics. Note that for TTF FETs, contrary to the case of TCNQ devices, conduction is observed for negative gate voltages because charge carriers are positively charged holes. Also, for TTF crystals, the background resistance in the off state is much larger than 1 GΩ. All measurements of FET characteristics were carried out at room temperature and in the vacuum (~10^{-6} mbar).

We have investigated more than 50 TTF–TCNQ interfaces by carrying out transport measurements in air, in vacuum and as a function of temperature. Whereas the resistance of individual TTF or TCNQ crystals is (much) larger than 1 GΩ at room temperature, for all TTF–TCNQ interfaces the value of resistance measured in a two-terminal configuration was typically lower than 100 kΩ. This value includes the contact resistance, which is in general large (Fig. 4a,b), and to measure the contribution of the TTF–TCNQ

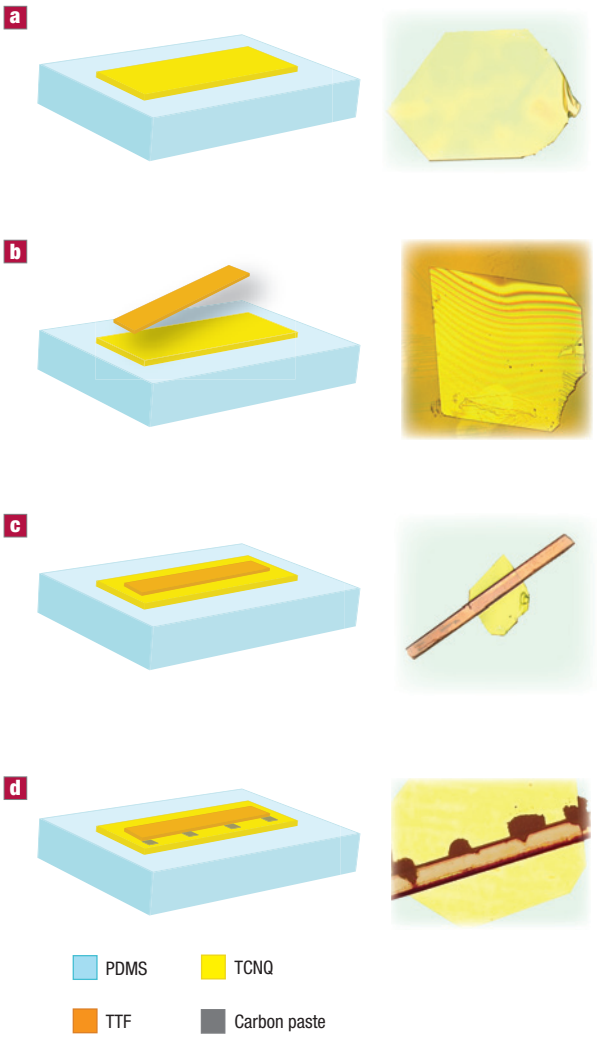

Figure 3 Assembly of TTF–TCNQ charge-transfer interfaces. The different steps followed to assemble TTF–TCNQ interfaces: schematic diagrams of the individual steps are shown in the left column and the corresponding optical microscope images in the right column. **a**, In the first step, a TCNQ single crystal is placed onto a PDMS substrate. **b**, A thin TTF crystal positioned on top spontaneously adheres to the TCNQ crystal. The interference fringes seen in the optical microscope image are characteristically observed during this adhesion process, and they disappear when the adhesion is complete. **c**, The result of the crystal bonding process. **d**, Electrical contacts to the interface are fabricated using a carbon paste consisting of a water-based suspension of amorphous carbon nanoparticles, which are deposited manually at the edge of the interface. Gold wires for electrical measurements are attached to the carbon paste using a solvent-free silver epoxy.

interface, it is essential to use a four-terminal configuration. Owing to the small size of the samples (typically ~500 μm linear dimension), we succeeded in attaching four contacts to only a fraction of the devices (approximately 15). From these devices, we found that the resistance-per-square of the TTF–TCNQ interface ranges from 1 kΩ per square to approximately 30 kΩ per square. The spread seems to be mainly related to the quality of the different devices, but, in part, it may also originate from anisotropy in the conduction. In fact, the lamination process used for the interface assembly does not give good control of the relative orientation of the two crystals, so that in different devices transport occurs along different crystalline directions (the mobility of charge carriers in organic crystals is known to be slightly anisotropic, typically a factor of 3–4, for materials with a molecular packing similar to that of TTF and TCNQ[21,28]). Note also that TTF–TCNQ interfaces were assembled using two different crystalline phases of TTF, which have different lattice constants (the α-phase and the β-phase; see the Methods section). High conductivity was observed in both cases, suggesting that its occurrence does not crucially depend on the commensurability of the TCNQ and TTF lattices. Finally, the conductivity values are essentially identical irrespective of whether measurements are carried out in air or in vacuum (Fig. 4c) and the interfaces were stable over long periods of time. This is illustrated in Fig. 4d, which shows that the conductivity does not change significantly over a period of months.

The measurements of the temperature dependence of the conductivity are of particular interest. For a two-dimensional conductor with a square resistance that varies from being much smaller than, to comparable or larger than the resistance quantum ($h/e^2 \sim 26\,\mathrm{k\Omega}$), a crossover in the observed temperature dependence should be expected[29]. Specifically, when the square resistance is high, electronic states tend to be localized and the interface becomes more resistive as the temperature is lowered. On the contrary, when the square resistance is much smaller than the quantum resistance, the resistance should decrease with decreasing temperature in a broad temperature range. Indeed, this is what is observed experimentally, as illustrated in Fig. 5c by measurements carried out on three different samples: the temperature dependence of the resistance of an interface with $R \sim 1\,\mathrm{k\Omega}$ per square decreases with decreasing temperature, whereas an interface with $R \sim 6\,\mathrm{k\Omega}$ per square at room temperature becomes more resistive on cooling. In total, we carried out temperature-dependent measurements on five interfaces with resistance smaller than 10 kΩ per square, all consistent with the data shown in Fig. 5c and with two of them exhibiting a metallic temperature dependence (two of these five samples could only be measured in a smaller temperature range, because the crystals cracked during cooling). We also measured other devices with a larger square resistance, which exhibited insulating behaviour, as expected.

Another key observation enabled by the temperature-dependent measurements is that no sharp resistance increase is seen throughout the entire temperature range. In particular, no special feature in the data is present at $T = 54\,\mathrm{K}$, where in bulk TTF–TCNQ the resistivity increases by a factor of 20 in a few kelvin range[10,11] owing to the occurrence of the first Peierls transition. Our data show unambiguously that, contrary to the bulk, such a transition does not occur at TTF–TCNQ interfaces. The absence of a Peierls transition enables us to conclude directly that the electronic properties of TTF–TCNQ interfaces are intrinsically different from those of bulk TTF–TCNQ. This excludes that the high conductivity measured at TTF–TCNQ interfaces originates from the formation of a bulk-like layer (possibly formed as a consequence of interdiffusion of the two molecules), in which case the effect of a Peierls transition should also be visible. This finding is consistent with the observed stability of our samples, because material interdiffusion would lead, after increasingly long periods of time, to an increasingly thicker conducting layer near the interface and, correspondingly, to a decrease in the measured resistance (which is not what we observe; see Fig. 4d). We conclude that at TTF–TCNQ interfaces, a metallic conductor is formed owing to charge transfer between the two molecules.

Having established the occurrence of metallic conductivity at TTF–TCNQ interfaces, we take a first step in the analysis of the interfacial electronic properties. An important aspect of bulk TTF–TCNQ is the negligible hybridization between the molecular orbitals of the TTF and of the TCNQ chains. As the molecular

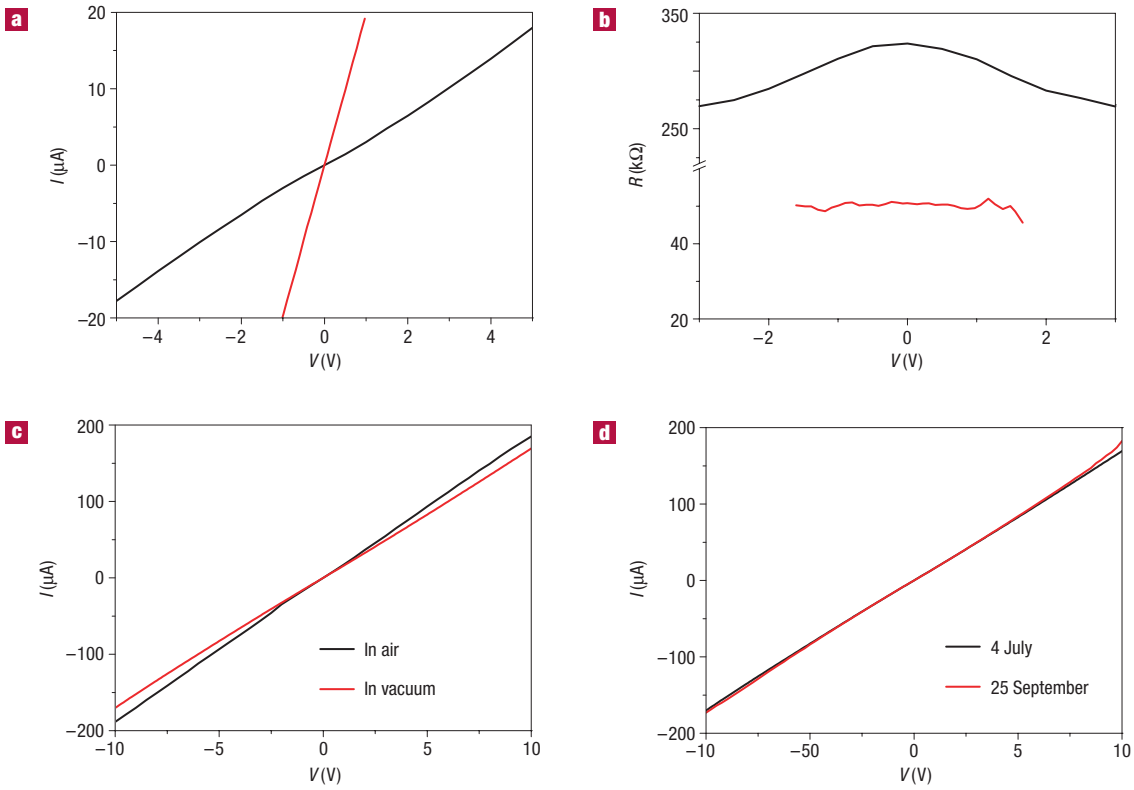

Figure 4 Room-temperature electrical characteristics of TTF–TCNQ interfaces. All interfaces that we have measured—more than 50—exhibit a large electrical conductance, typically six orders of magnitude (or more) larger than the conductance of the individual TTF and TCNQ crystals. **a**, A comparison between the *I–V* curves measured on the same device, in a two-terminal (black curve) and four-terminal (red curve) configuration. As can be seen, the contact resistance is in general large, and it typically results in a characteristic nonlinearity at low bias. **b**, The nonlinearity is more clearly visible in the differential resistance and is completely absent in the four-terminal measurements. **c**, A high conductance is observed irrespective of whether measurements are carried out in air or in vacuum. **d**, The TTF–TCNQ interfaces assembled by lamination are very stable; no difference is observed in the measurements carried out almost three months after fabrication.

planes are already very weakly coupled within individual crystals of TTF and TCNQ, it is likely that the coupling between the adjacent TTF and TCNQ planes at the TTF–TCNQ interface is also weak, that is, the hybridization between orbitals of the two molecules is likely to be very small in this case as well. It follows that the interfacial conductivity that we observe is due to two decoupled conducting layers with equal and opposite amounts of charge: one in which conduction is due to holes in the HOMO band of TTF, and the other in which current is carried by electrons in the conduction band of TCNQ. With the surface density of TTF and TCNQ molecules being approximately 5×10^{14} cm^{-2}, and assuming the amount of charge transferred from TTF to TCNQ at the interface to be approximately the same as in the bulk (0.59 electron charges per molecule[10,11]), we obtain a square resistance of $\sim$1 kΩ for mobility values of a few cm^2 V^{-1} s^{-1} at room temperature (entirely realistic in our crystals). This value compares unexpectedly well with the square resistance that we measure in our best samples (the high resistance values measured in other samples can have many different origins, such as a non-uniform adhesion of the crystals or the presence of defects reducing the mobility). The absence of a Peierls transition at the interface is also easy to understand. In fact, in crystals of conjugated molecules[12] with a structure that is similar to that of TTF and of TCNQ, only a small inplane anisotropy of the carrier is observed experimentally[21,28]. This implies that the electron and holes at the surface of the TCNQ and TTF crystals are not confined to move along one-dimensional chains, as happens in bulk TTF–TCNQ. Finally, with the surface charge density being larger than 10^{14} carriers cm^{-2}, the Thomas–Fermi screening length is comparable to or smaller than the size of a molecule. As a consequence, the electron and holes at the TTF–TCNQ interface do not penetrate significantly in the bulk of the organic crystals, and the conducting layer is only a few molecules thick.

Given the similarity of TTF and TCNQ to other conjugated molecules used in plastic electronics, it is interesting to compare our results with existing work on other related systems, in which electronic transport also takes place at the surface of organic materials. In organic FETs, for instance, the lowest resistivity measured so far is of the order of 100 kΩ per square—between one and two orders of magnitude larger than the resistivity values reported here. These values are attained at a surface carrier density between 1 and 5×10^{13} carriers cm^{-2}, at mobility values around a few cm^2 V^{-1} s^{-1} (ref. 30). Because in our TTF and TCNQ crystals the mobility is of comparable magnitude, the much lower resistivity of TTF–TCNQ interfaces originates from a much higher density of charge carriers. Indeed, our estimate of $\sim 5 \times 10^{14}$ carriers cm^{-2} (see above) is between one and two orders of magnitude larger than the largest carrier densities attained in FETs. Similar considerations hold true for structures in which charge transfer from other molecules was previously used to control the surface density of charge carriers. One example is provided by organic FETs in which self-assembled monolayers chemically bonded to the gate dielectric are used to tune the threshold voltage (see, for example, ref. 31).

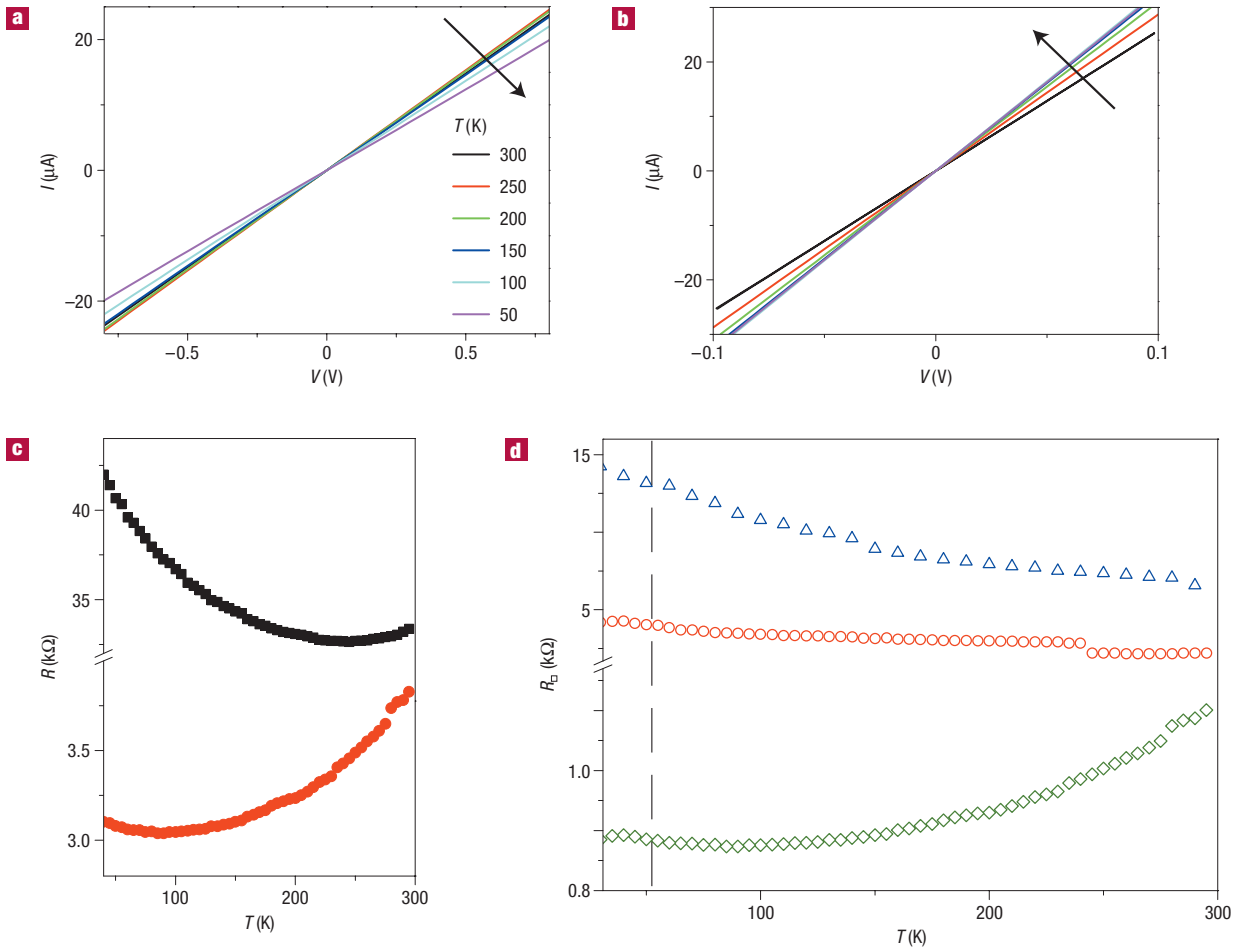

Figure 5 Temperature dependence of the electrical characteristics of TTF–TCNQ interfaces. The temperature dependence of the electrical characteristics of TTF–TCNQ interfaces is studied by measuring their *I*–*V* curves in the range between 40 and 300 K. **a**,**b**, The evolution of the temperature dependence of the *I*–*V* curves measured in a two-terminal (**a**) and four-terminal (**b**) configuration. The arrows indicate the variation in current with decreasing *T*. **c**, The full temperature dependence of the resistance. In a two-terminal configuration, the resistance is always observed to increase with decreasing temperature, contrary to what is observed in four-terminal measurements. **d**, The temperature dependence of the resistance-per-square, measured in a four-terminal configuration, in three different samples. The increase in resistance with decreasing temperature that is observed in devices with larger square resistance crosses over smoothly into a metallic behaviour (decrease of resistance with decreasing temperature) for devices where the square resistance is sufficiently low. The crossover occurs when the resistance-per-square is approximately 4–5 kΩ, of the order of the resistance quantum. The vertical line at $T = 54$ K represents the temperature at which a charge density wave transition is observed in bulk TTF–TCNQ, causing the resistance to increase by a factor of 20 in a range of a few degrees kelvin. In all of our devices, no indication of a resistance increase is visible around this temperature, illustrating the role of the different dimensionality of interfaces as compared with TTF–TCNQ bulk.

The amount of charge transferred by this technique, however, is low, typically a few 10^{12} carriers cm^{-2}. Much higher carrier densities have recently been achieved by direct chemical bonding of a self-assembled monolayer onto the surface of rubrene crystals[5]. Still, also in this case, both the carrier density and the conductivity were found to be between one and two orders of magnitude lower than in TTF–TCNQ charge-transfer interfaces. Overall, therefore, the comparison between the conductivity at the surface of organic materials measured in different configurations and that of TTF–TCNQ interfaces quantitatively supports our conclusion that in this latter system the carrier density is much higher.

More generally, the electron–hole metallic conductor that is formed at the TTF–TCNQ interface is a new type of electronic system. We believe that in charge-transfer interfaces of this kind (based on TTF and TCNQ or on other similar pairs of conjugated organic molecules), new physical phenomena may appear owing to electron correlations, which in organic materials are known to be strong owing to the narrow electronic bandwidth. For instance, in quasi-two-dimensional organic charge-transfer salts based on the bis(ethylenedithio)-TTF molecule, superconductivity occurs at temperature as high as 10 K at ambient pressure[11]. As bis(ethylenedithio)-TTF-based materials are formed by stacked molecular planes that are electronically decoupled, it seems definitely possible that superconductivity will also occur at charge-transfer interfaces assembled in the way described here. Another interesting electronic state that could be formed at low temperature is an excitonic insulator[32], which is predicted to be realized in systems consisting of an electron and one hole layer closely facing each other with a negligible probability of interlayer tunnelling (precisely as in our TTF–TCNQ interfaces). Next to these specific examples, the virtually infinite classes of organic molecules that can be used to assemble molecular interfaces suggests that organic

charge-transfer interfaces will offer an unprecedented versatility for the realization of two-dimensional conductors with tunable electronic properties (for example, molecules with spin could be used to induce and control magnetic phenomena). In the field of organic charge-transfer salts, a myriad of molecules have been synthesized over the past two decades to control the properties of new molecular materials, often to find that the co-crystallization of these molecules in a single compound is extremely challenging or prohibitively difficult. Working with interfaces—rather than with bulk materials—has the potential to solve this problem.

METHODS

TCNQ crystals were grown by a vapour phase transport method commonly used for organic materials[33], with argon as a carrier gas, at ambient pressure. TTF crystals were grown both from vapour phase and from solution. For this material, vapour phase growth is possible under mild vacuum (~1 mbar), which is needed to lower the temperature required to sublime TTF molecules at a sufficient rate, without inducing chemical decomposition. β-phase single TTF crystals are obtained in this way. TTF crystals were also grown from solution by dispersing 150 mg of material in 50 ml of *n*-hexane, and letting the solvent evaporate slowly over the course of two weeks. In this way, α-TTF crystal are obtained. Both α- and β-TTF–TCNQ interfaces are highly conducting, but from the statistical analysis of our results, it seems that α-phase TTF–TCNQ interfaces exhibit on average slightly higher conductivity than β-phase TTF–TCNQ interfaces. It is currently unclear if this difference is due to an intrinsic property of the interface or from other factors such as, for instance, differences in the adhesion of the crystals.

As mentioned in the text, the interfaces are mounted on a PDMS support. The use of PDMS—as opposed to a rigid substrate such as glass or silicon—is essential to carry out low-temperature measurements below 200 K. In fact, when mounted on rigid substrates, the crystals crack on cooling, owing to the different thermal expansion coefficients of the molecular materials and of the substrate. Electrical contact to the interfacial conducting layer is achieved by using a conducting carbon paste consisting of a water-based suspension of carbon nanoparticles, which is manually deposited (under an optical microscope) at the edges of the two crystals, to wet the interface. With practice, this technique enables the fabrication of a contact with size smaller than 50 μm. A 25 μm gold wire is subsequently attached to the carbon paste protruding away from the interface using a solvent-free silver epoxy, and connected to the (standard) chip carrier onto which the devices are mounted.

Electrical measurements were done both in air and in the vacuum chamber of a flow cryostat with essentially identical results, using either an HP 4156A or an Agilent Technologies E5270B parameter analyser. Measurements as a function of temperature require very slow cooling, because large and abrupt changes in temperature can result in the formation of cracks in the crystals, even when the crystals are mounted on PDMS supports. In practice, we often took an entire day to measure I–V curves of a device down to the lowest temperature in the experiments, starting from room temperature. In the cryostat that we have used to ensure sufficiently low cooling rates, non-ideal radiation shielding from the cryostat walls prevents the sample temperature from being lowered below 40 K. Future experiments will aim at reaching lower temperatures and at applying a large magnetic field.

Received 25 March 2008; accepted 12 May 2008; published 15 June 2008.

References

1. Chiang, C. K. *et al.* Electrical conductivity in doped polyacetylene. *Phys. Rev. Lett.* **39**, 1098–1101 (1977).
2. Haddon, R. C. *et al.* Conducting films of C_{60} and C_{70} by alkali-metal doping. *Nature* **350**, 320–322 (1991).
3. Hebard, A. F. *et al.* Superconductivity at 18 K in potassium-doped C_{60}. *Nature* **350**, 600–601 (1991).
4. Jerome, D. & Schulz, H. J. Organic conductors and superconductors. *Adv. Phys.* **31**, 299–490 (1982).
5. Calhoun, M. F., Sanchez, J., Olaya, D., Gershenson, M. E. & Podzorov, V. Electronic functionalization of the surface of organic semiconductors with self-assembled monolayers. *Nature Mater.* **7**, 84–89 (2008).
6. Ohtomo, A. & Hwang, H. Y. A high-mobility electron gas at the $LaAlO_3/SrTiO_3$ heterointerface. *Nature* **427**, 423–426 (2004).
7. Reyren, N. *et al.* Superconducting interfaces between insulating oxides. *Science* **317**, 1196–1199 (2007).
8. Brinkman, A. *et al.* Magnetic effects at the interface between non-magnetic oxides. *Nature Mater.* **6**, 493–496 (2007).
9. Ferraris, J., Walatka, V., Perlstei, J. H. & Cowan, D. O. Electron-transfer in a new highly-conducting donor–acceptor complex. *J. Am. Chem. Soc.* **95**, 948–949 (1973).
10. Jerome, D. Organic conductors: from charge density wave TTF–TCNQ to superconducting $(TMTSF)_2PF_6$. *Chem. Rev.* **104**, 5565–5591 (2004).
11. Ishiguro, T., Yamaji, K. & Saito, G. *Organic Superconductors* 2nd edn (Springer, Berlin, 1998).
12. Silinsh, E. A. & Capek, V. *Organic Molecular Crystals* (American Institute of Physics, New York, 1994).
13. Farges, J. P. & Brau, A. Electrical properties of powdered or pure TCNQ and TTF: Evidence for a strong solid-state charge-transfer reaction. *Physica* **143B**, 324–326 (1986).
14. de Boer, R. W. I., Gershenson, M. E., Morpurgo, A. F. & Podzorov, V. Organic single-crystal field-effect transistors. *Phys. Status Solidi. A* **201**, 1302–1331 (2004).
15. Aleshin, A. N., Lee, J. Y., Chu, S. W., Kim, J. S. & Park, Y. W. Mobility studies of field-effect transistor structures based on anthracene single crystals. *Appl. Phys. Lett.* **84**, 5383–5385 (2004).
16. de Boer, R. W. I., Klapwijk, T. M. & Morpurgo, A. F. Field-effect transistors on tetracene single crystals. *Appl. Phys. Lett.* **83**, 4345–4347 (2003).
17. Takeya, J. *et al.* Field-induced charge transport at the surface of pentacene single crystals: A method to study charge dynamics of two dimensional electron systems in organic crystals. *J. Appl. Phys.* **94**, 5800–5804 (2003).
18. Hulea, I. N. *et al.* Tunable Frohlich polarons in organic single-crystal transistors. *Nature Mater.* **5**, 982–986 (2006).
19. de Boer, R. W. I. *et al.* Ambipolar Cu- and Fe-phthalocyanine single-crystal field-effect transistors. *Appl. Phys. Lett.* **86**, 262109 (2005).
20. Horowitz, G., Garnier, F., Yassar, A., Hajlaoui, R. & Kouki, F. Field-effect transistor made with a sexithiophene single crystal. *Adv. Mater.* **8**, 52–54 (1996).
21. Sundar, V. C. *et al.* Elastomeric transistor stamps: Reversible probing of charge transport in organic crystals. *Science* **303**, 1644–1646 (2004).
22. Molinari, A., Gutierrez, I., Hulea, I. N., Russo, S. & Morpurgo, A. F. Bias-dependent contact resistance in rubrene single-crystal field-effect transistors. *Appl. Phys. Lett.* **90**, 212103 (2007).
23. Takahasi, T., Takenobu, T., Takeya, J. & Iwasa, Y. Ambipolar organic field-effect transistors based on rubrene single crystals. *Appl. Phys. Lett.* **88**, 033505 (2006).
24. Takeya, J., Yamagishi, M., Tominari, Y. & Nakazawa, Y. Gate dielectric materials for high-mobility organic transistors of molecular semiconductor crystals. *Solid State Electron.* **51**, 1338–1343 (2007).
25. Menard, E. *et al.* Nanoscale surface morphology and rectifying behavior of a bulk single-crystal organic semiconductor. *Adv. Mater.* **18**, 1552–1556 (2006).
26. Gershenson, M. E., Podzorov, V. & Morpurgo, A. F. Electronic transport in single-crystal organic transistors. *Rev. Mod. Phys.* **78**, 973–989 (2006).
27. Hulea, I. N., Russo, S., Molinari, A. & Morpurgo, A. F. Reproducible low contact resistance in rubrene single-crystal field-effect transistors with nickel electrodes. *Appl. Phys. Lett.* **88**, 113512 (2006).
28. Guo, D., Sakamoto, K., Miki, K., Ikeda, S. & Saiki, K. Orientation control of pentacene and transport anisotropy of the thin film transistor by photoaligned polyimide film. *Appl. Phys. Lett.* **90**, 102117 (2007).
29. Lee, P. A. & Ramakrishnan, T. V. Disordered electronic systems. *Rev. Mod. Phys.* **57**, 287–337 (1985).
30. Fratini, S., Xie, H., Hulea, I. N., Ciuchi, S. & Morpurgo, A. F. Current saturation and Coulomb interactions in organic single-crystal transistors. *New J. Phys.* **10**, 033031 (2008).
31. Kobayashi, S. *et al.* Control of carrier density by self-assembled monolayers in organic field-effect transistors. *Nature Mater.* **3**, 317–322 (2004).
32. Jerome, D., Rice, T. M. & Kohn, W. Excitonic insulator. *Phys. Rev.* **158**, 462–475 (1967).
33. Laudise, R. A., Kloc, C., Simpkins, P. G. & Sigriest, T. Physical vapor growth of organic crystals. *J. Cryst. Growth* **187**, 449–454 (1998).
34. Kistenmacher, T. J., Phillips, T. E. & Cowan, D. O. The crystal structure of the 1:1 radical cation-radical anion salt of 2-2′-bis-1,3-dithiole (TTF) and 7,7,8,8-tetracyanoquinodimethane (TCNQ). *Acta Crystallogr. B* **30**, 763–768 (1974).
35. Cooper, W. F. *et al.* Crystal and molecular structure of aromatic sulphur compound 2,2′-bi-1,3-dithiole—evidence for *d*-orbital participation in bonding. *J. Chem. Soc. D* **16**, 889–890 (1971).
36. Long, R. E., Sparks, R. A. & Trueblood, K. N. The crystal and molecular structure of 7,7,8,8-tetracyanoquinodimethane. *Acta Crystallogr.* **18**, 932–939 (1965).
37. Menard, E. *et al.* High-performance n- and p-type single-crystal organic transistors with free-space gate dielectrics. *Adv. Mater.* **16**, 2097–2101 (2004).

Acknowledgements

A.F.M. gratefully acknowledges a useful conversation with D. van der Marel. H.A. acknowledges FCT for financial support under contract nr. SFRH/BPD/34333/2006. Financial support from NanoNed and NWO is also acknowledged.

Author contributions

H.A. grew the molecular crystals, fabricated the devices and took part in the electrical measurements; A.S.M. carried out most of the electrical measurements on TTF–TCNQ interfaces; H.X. did the field-effect transistor characterization of TTF and TCNQ crystals; A.F.M. conceived the experiments, directed the research and wrote the manuscript.

Author information

Reprints and permission information is available online at http://npg.nature.com/reprintsandpermissions. Correspondence and requests for materials should be addressed to A.F.M.